

CERN-PH-EP-2014-204  
12 August 2014

**Odd and Even Partial Waves of  $\eta\pi^-$  and  $\eta'\pi^-$  in  $\pi^-p \rightarrow \eta^{(\prime)}\pi^-p$  at  
191 GeV/c**

The COMPASS Collaboration

**Abstract**

Exclusive production of  $\eta\pi^-$  and  $\eta'\pi^-$  has been studied with a 191 GeV/c  $\pi^-$  beam impinging on a hydrogen target at COMPASS (CERN). Partial-wave analyses reveal different odd/even angular momentum ( $L$ ) characteristics in the inspected invariant mass range up to 3 GeV/c<sup>2</sup>. A striking similarity between the two systems is observed for the  $L = 2, 4, 6$  intensities (scaled by kinematical factors) and the relative phases. The known resonances  $a_2(1320)$  and  $a_4(2040)$  are in line with this similarity. In contrast, a strong enhancement of  $\eta'\pi^-$  over  $\eta\pi^-$  is found for the  $L = 1, 3, 5$  waves, which carry non- $q\bar{q}$  quantum numbers. The  $L = 1$  intensity peaks at 1.7 GeV/c<sup>2</sup> in  $\eta'\pi^-$  and at 1.4 GeV/c<sup>2</sup> in  $\eta\pi^-$ , the corresponding phase motions with respect to  $L = 2$  are different.

*(to be submitted to Phys. Lett. B)*

## The COMPASS Collaboration

C. Adolph<sup>8</sup>, R. Akhunzyanov<sup>7</sup>, M.G. Alexeev<sup>27</sup>, G.D. Alexeev<sup>7</sup>, A. Amoroso<sup>27,29</sup>, V. Andrieux<sup>22</sup>, V. Anosov<sup>7</sup>, A. Austregesilo<sup>10,17</sup>, B. Badełek<sup>31</sup>, F. Balestra<sup>27,29</sup>, J. Barth<sup>4</sup>, G. Baum<sup>1</sup>, R. Beck<sup>3</sup>, Y. Bedfer<sup>22</sup>, A. Berlin<sup>2</sup>, J. Bernhard<sup>13</sup>, K. Bicker<sup>10,17</sup>, E. R. Bielert<sup>10</sup>, J. Bieling<sup>4</sup>, R. Birsa<sup>25</sup>, J. Bisplinghoff<sup>3</sup>, M. Bodlak<sup>19</sup>, M. Boer<sup>22</sup>, P. Bordalo<sup>12,a</sup>, F. Bradamante<sup>24,25</sup>, C. Braun<sup>8</sup>, A. Bressan<sup>24,25</sup>, M. Büchele<sup>9</sup>, E. Burtin<sup>22</sup>, L. Capozza<sup>22</sup>, M. Chiosso<sup>27,29</sup>, S.U. Chung<sup>17,b</sup>, A. Cicuttin<sup>26,25</sup>, M.L. Crespo<sup>26,25</sup>, Q. Curiel<sup>22</sup>, S. Dalla Torre<sup>25</sup>, S.S. Dasgupta<sup>6</sup>, S. Dasgupta<sup>25</sup>, O.Yu. Denisov<sup>29</sup>, S.V. Donskov<sup>21</sup>, N. Doshita<sup>33</sup>, V. Duic<sup>24</sup>, W. Dünneweber<sup>16</sup>, M. Dzierwiecki<sup>32</sup>, A. Efremov<sup>7</sup>, C. Elia<sup>24,25</sup>, P.D. Eversheim<sup>3</sup>, W. Eyrich<sup>8</sup>, M. Faessler<sup>16</sup>, A. Ferrero<sup>22</sup>, M. Finger<sup>19</sup>, M. Finger jr.<sup>19</sup>, H. Fischer<sup>9</sup>, C. Franco<sup>12</sup>, N. du Fresne von Hohenesche<sup>13,10</sup>, J.M. Friedrich<sup>17</sup>, V. Frolov<sup>10</sup>, F. Gautheron<sup>2</sup>, O.P. Gavrichtchouk<sup>7</sup>, S. Gerassimov<sup>15,17</sup>, R. Geyer<sup>16</sup>, I. Gnesi<sup>27,29</sup>, B. Gobbo<sup>25</sup>, S. Goertz<sup>4</sup>, M. Gorzellik<sup>9</sup>, S. Grabmüller<sup>17</sup>, A. Grasso<sup>27,29</sup>, B. Grube<sup>17</sup>, T. Grussenmeyer<sup>9</sup>, A. Guskov<sup>7</sup>, F. Haas<sup>17</sup>, D. von Harrach<sup>13</sup>, D. Hahne<sup>4</sup>, R. Hashimoto<sup>33</sup>, F.H. Heinsius<sup>9</sup>, F. Herrmann<sup>9</sup>, F. Hinterberger<sup>3</sup>, Ch. Höppner<sup>17</sup>, N. Horikawa<sup>18,d</sup>, N. d'Hose<sup>22</sup>, S. Huber<sup>17</sup>, S. Ishimoto<sup>33,e</sup>, A. Ivanov<sup>7</sup>, Yu. Ivanshin<sup>7</sup>, T. Iwata<sup>33</sup>, R. Jahn<sup>3</sup>, V. Jary<sup>20</sup>, P. Jasinski<sup>13</sup>, P. Jörg<sup>9</sup>, R. Joosten<sup>3</sup>, E. Kabuß<sup>13</sup>, B. Ketzer<sup>17,f</sup>, G.V. Khaustov<sup>21</sup>, Yu.A. Khokhlov<sup>21,g</sup>, Yu. Kisselev<sup>7</sup>, F. Klein<sup>4</sup>, K. Klimaszewski<sup>30</sup>, J.H. Koivuniemi<sup>2</sup>, V.N. Kolosov<sup>21</sup>, K. Kondo<sup>33</sup>, K. Königsman<sup>9</sup>, I. Konorov<sup>15,17</sup>, V.F. Konstantinov<sup>21</sup>, A.M. Kotzinian<sup>27,29</sup>, O. Kouznetsov<sup>7</sup>, M. Krämer<sup>17</sup>, Z.V. Kroumchtein<sup>7</sup>, N. Kuchinski<sup>7</sup>, F. Kunne<sup>22</sup>, K. Kurek<sup>30</sup>, R.P. Kurjata<sup>32</sup>, A.A. Lednev<sup>21</sup>, A. Lehmann<sup>8</sup>, M. Levillain<sup>22</sup>, S. Levorato<sup>25</sup>, J. Lichtenstadt<sup>23</sup>, A. Maggiora<sup>29</sup>, A. Magnon<sup>22</sup>, N. Makke<sup>24,25</sup>, G.K. Mallot<sup>10</sup>, C. Marchand<sup>22</sup>, A. Martin<sup>24,25</sup>, J. Marzec<sup>32</sup>, J. Matousek<sup>19</sup>, H. Matsuda<sup>33</sup>, T. Matsuda<sup>14</sup>, G. Meshcheryakov<sup>7</sup>, W. Meyer<sup>2</sup>, T. Michigami<sup>33</sup>, Yu.V. Mikhailov<sup>21</sup>, Y. Miyachi<sup>33</sup>, A. Nagaytsev<sup>7</sup>, T. Nagel<sup>17</sup>, F. Nerling<sup>13</sup>, S. Neubert<sup>17</sup>, D. Neyret<sup>22</sup>, J. Novy<sup>20</sup>, W.-D. Nowak<sup>9</sup>, A.S. Nunes<sup>12</sup>, A.G. Olshevsky<sup>7</sup>, I. Orlov<sup>7</sup>, M. Ostrick<sup>13</sup>, R. Panknin<sup>4</sup>, D. Panzieri<sup>28,29</sup>, B. Parsamyan<sup>27,29</sup>, S. Paul<sup>17</sup>, D.V. Peshekhonov<sup>7</sup>, S. Platchkov<sup>22</sup>, J. Pochodzalla<sup>13</sup>, V.A. Polyakov<sup>21</sup>, J. Pretz<sup>4,h</sup>, M. Quaresma<sup>12</sup>, C. Quintans<sup>12</sup>, S. Ramos<sup>12,a</sup>, C. Regali<sup>9</sup>, G. Reicherz<sup>2</sup>, E. Rocco<sup>10</sup>, N.S. Rossiyskaya<sup>7</sup>, D.I. Ryabchikov<sup>21</sup>, A. Rychter<sup>32</sup>, V.D. Samoylenko<sup>21</sup>, A. Sandacz<sup>30</sup>, S. Sarkar<sup>6</sup>, I.A. Savin<sup>7</sup>, G. Sbrizzai<sup>24,25</sup>, P. Schiavon<sup>24,25</sup>, C. Schill<sup>9</sup>, T. Schlüter<sup>16</sup>, K. Schmidt<sup>9,c</sup>, H. Schmieden<sup>4</sup>, K. Schönning<sup>10</sup>, S. Schopferer<sup>9</sup>, M. Schott<sup>10</sup>, O.Yu. Shevchenko<sup>7,\*</sup>, L. Silva<sup>12</sup>, L. Sinha<sup>6</sup>, S. Sirtl<sup>9</sup>, M. Slunicka<sup>7</sup>, S. Sosio<sup>27,29</sup>, F. Sozzi<sup>25</sup>, A. Srnka<sup>5</sup>, L. Steiger<sup>25</sup>, M. Stolarski<sup>12</sup>, M. Sulc<sup>11</sup>, R. Sulej<sup>30</sup>, H. Suzuki<sup>33,d</sup>, A. Szabelski<sup>30</sup>, T. Szameitat<sup>9,c</sup>, P. Sznajder<sup>30</sup>, S. Takekawa<sup>27,29</sup>, J. ter Wolbeek<sup>9,c</sup>, S. Tessaro<sup>25</sup>, F. Tessarotto<sup>25</sup>, F. Thibaud<sup>22</sup>, S. Uhl<sup>17</sup>, I. Uman<sup>16</sup>, M. Virius<sup>20</sup>, L. Wang<sup>2</sup>, T. Weisrock<sup>13</sup>, M. Wilfert<sup>13</sup>, R. Windmolders<sup>4</sup>, H. Wollny<sup>22</sup>, K. Zarembo<sup>32</sup>, M. Zavertyaev<sup>15</sup>, E. Zemlyanichkina<sup>7</sup>, M. Ziembicki<sup>32</sup> and A. Zink<sup>8</sup>

<sup>1</sup> Universität Bielefeld, Fakultät für Physik, 33501 Bielefeld, Germany<sup>i</sup>

<sup>2</sup> Universität Bochum, Institut für Experimentalphysik, 44780 Bochum, Germany<sup>iP</sup>

<sup>3</sup> Universität Bonn, Helmholtz-Institut für Strahlen- und Kernphysik, 53115 Bonn, Germany<sup>i</sup>

<sup>4</sup> Universität Bonn, Physikalisches Institut, 53115 Bonn, Germany<sup>i</sup>

<sup>5</sup> Institute of Scientific Instruments, AS CR, 61264 Brno, Czech Republic<sup>j</sup>

<sup>6</sup> Matrivani Institute of Experimental Research & Education, Calcutta-700 030, India<sup>k</sup>

<sup>7</sup> Joint Institute for Nuclear Research, 141980 Dubna, Moscow region, Russia<sup>l</sup>

<sup>8</sup> Universität Erlangen–Nürnberg, Physikalisches Institut, 91054 Erlangen, Germany<sup>i</sup>

<sup>9</sup> Universität Freiburg, Physikalisches Institut, 79104 Freiburg, Germany<sup>iP</sup>

<sup>10</sup> CERN, 1211 Geneva 23, Switzerland

<sup>11</sup> Technical University in Liberec, 46117 Liberec, Czech Republic<sup>j</sup>

<sup>12</sup> LIP, 1000-149 Lisbon, Portugal<sup>m</sup>

<sup>13</sup> Universität Mainz, Institut für Kernphysik, 55099 Mainz, Germany<sup>i</sup>

<sup>14</sup> University of Miyazaki, Miyazaki 889-2192, Japan<sup>n</sup>

- <sup>15</sup> Lebedev Physical Institute, 119991 Moscow, Russia
- <sup>16</sup> Ludwig-Maximilians-Universität München, Department für Physik, 80799 Munich, Germany<sup>io</sup>
- <sup>17</sup> Technische Universität München, Physik Department, 85748 Garching, Germany<sup>io</sup>
- <sup>18</sup> Nagoya University, 464 Nagoya, Japan<sup>n</sup>
- <sup>19</sup> Charles University in Prague, Faculty of Mathematics and Physics, 18000 Prague, Czech Republic<sup>j</sup>
- <sup>20</sup> Czech Technical University in Prague, 16636 Prague, Czech Republic<sup>j</sup>
- <sup>21</sup> State Scientific Center Institute for High Energy Physics of National Research Center ‘Kurchatov Institute’, 142281 Protvino, Russia
- <sup>22</sup> CEA IRFU/SPhN Saclay, 91191 Gif-sur-Yvette, France<sup>p</sup>
- <sup>23</sup> Tel Aviv University, School of Physics and Astronomy, 69978 Tel Aviv, Israel<sup>q</sup>
- <sup>24</sup> University of Trieste, Department of Physics, 34127 Trieste, Italy
- <sup>25</sup> Trieste Section of INFN, 34127 Trieste, Italy
- <sup>26</sup> Abdus Salam ICTP, 34151 Trieste, Italy
- <sup>27</sup> University of Turin, Department of Physics, 10125 Turin, Italy
- <sup>28</sup> University of Eastern Piedmont, 15100 Alessandria, Italy
- <sup>29</sup> Torino Section of INFN, 10125 Turin, Italy
- <sup>30</sup> National Centre for Nuclear Research, 00-681 Warsaw, Poland<sup>r</sup>
- <sup>31</sup> University of Warsaw, Faculty of Physics, 00-681 Warsaw, Poland<sup>r</sup>
- <sup>32</sup> Warsaw University of Technology, Institute of Radioelectronics, 00-665 Warsaw, Poland<sup>r</sup>
- <sup>33</sup> Yamagata University, Yamagata, 992-8510 Japan<sup>n</sup>
- <sup>a</sup> Also at Instituto Superior Técnico, Universidade de Lisboa, Lisbon, Portugal
- <sup>b</sup> Also at Department of Physics, Pusan National University, Busan 609-735, Republic of Korea and at Physics Department, Brookhaven National Laboratory, Upton, NY 11973, U.S.A.
- <sup>c</sup> Supported by the DFG Research Training Group Programme 1102 “Physics at Hadron Accelerators”
- <sup>d</sup> Also at Chubu University, Kasugai, Aichi, 487-8501 Japan<sup>n</sup>
- <sup>e</sup> Also at KEK, 1-1 Oho, Tsukuba, Ibaraki, 305-0801 Japan
- <sup>f</sup> Present address: Universität Bonn, Helmholtz-Institut für Strahlen- und Kernphysik, 53115 Bonn, Germany
- <sup>g</sup> Also at Moscow Institute of Physics and Technology, Moscow Region, 141700, Russia
- <sup>h</sup> present address: RWTH Aachen University, III. Physikalisches Institut, 52056 Aachen, Germany
- <sup>i</sup> Supported by the German Bundesministerium für Bildung und Forschung
- <sup>j</sup> Supported by Czech Republic MEYS Grants ME492 and LA242
- <sup>k</sup> Supported by SAIL (CSR), Govt. of India
- <sup>l</sup> Supported by CERN-RFBR Grants 08-02-91009 and 12-02-91500
- <sup>m</sup> Supported by the Portuguese FCT - Fundação para a Ciência e Tecnologia, COMPETE and QREN, Grants CERN/FP/109323/2009, CERN/FP/116376/2010 and CERN/FP/123600/2011
- <sup>n</sup> Supported by the MEXT and the JSPS under the Grants No.18002006, No.20540299 and No.18540281; Daiko Foundation and Yamada Foundation
- <sup>o</sup> Supported by the DFG cluster of excellence ‘Origin and Structure of the Universe’ (www.universe-cluster.de)
- <sup>p</sup> Supported by EU FP7 (HadronPhysics3, Grant Agreement number 283286)
- <sup>q</sup> Supported by the Israel Science Foundation, founded by the Israel Academy of Sciences and Humanities
- <sup>r</sup> Supported by the Polish NCN Grant DEC-2011/01/M/ST2/02350
- \* Deceased

The  $\eta\pi$  and  $\eta'\pi$  mesonic systems are attractive for spectroscopic studies because any state with odd angular momentum  $L$ , which coincides with the total spin  $J$ , has non- $q\bar{q}$  (“exotic”) quantum numbers  $J^{PC} = 1^{-+}, 3^{-+}, 5^{-+}, \dots$ . The  $1^{-+}$  state has been the principal case studied so far [1, 2].

A comparison of  $\eta\pi$  and  $\eta'\pi$  should illuminate the role of flavour symmetry. Since  $\eta$  and  $\eta'$  are dominantly flavour octet and singlet states, respectively, different  $SU(3)_{\text{flavour}}$  configurations are formed by  $\eta\pi$  and  $\eta'\pi$ . These configurations are linked to odd or even  $L$  by Bose symmetry [3–5]. Indeed, experimentally the diffractively produced  $P$ -wave ( $L = J = 1$ ) in  $\eta'\pi^-$  was found to be more pronounced than in  $\eta\pi^-$  [6]. A more systematic study of the two systems in the odd and even partial waves is desirable.

Diffractive production of  $\eta\pi^-$  and  $\eta'\pi^-$  was studied by previous experiments with  $\pi^-$  beams in the 18 GeV/ $c$ –37 GeV/ $c$  range [6–9]. Apart from the well-known resonances  $a_2(1320)$  and  $a_4(2040)$ , resonance features were observed for the exotic  $P$ -wave in the 1.4 GeV/ $c^2$  – 1.7 GeV/ $c^2$  mass range. It has quantum numbers  $J^{PG} = 1^{-}$ , where  $G$ -parity is used for the charged system, corresponding to  $C = +1$  since the isospin is 1. Results for charge-exchange production of  $\eta^{(\prime)}\pi^0$  are difficult to relate to these observations [1]. Critical discussions of the resonance character concern a possible dynamical origin of the behaviour of the  $L = 1$  wave in these systems [1, 10, 11].

The present study is performed with a 191 GeV/ $c$   $\pi^-$  beam and in the region  $0.1 (\text{GeV}/c)^2 < -t < 1 (\text{GeV}/c)^2$ , where  $t$  denotes the squared four-momentum transfer to the proton target. This is within the range of Reggeon-exchange processes [12, 13], where diffractive excitation and mid-rapidity (“central”) production coexist. The former can induce exclusive resonance production. The latter will lead to a system of the leading and the centrally produced mesons with (almost) no interaction in the final state.

In this Letter, the behaviour of all partial waves with  $L = 1 - 6$  in the  $\eta^{(\prime)}\pi^-$  invariant mass range up to 3 GeV/ $c^2$  is studied. A peculiar difference between  $\eta\pi^-$  and  $\eta'\pi^-$  in the even and odd- $L$  waves is observed.

The data were collected with the COMPASS apparatus at CERN. COMPASS is a two-stage magnetic spectrometer with tracking and calorimetry in both stages [14, 15]. A beam of negatively charged hadrons at 191 GeV/ $c$  was impinging on a liquid hydrogen target of 40 cm length and 35 mm diameter. Using the information from beam particle identification detectors, it was checked that  $K^-$  and  $\bar{p}$  admixtures to the 97%  $\pi^-$  beam are insignificant in the final sample analysed here. Recoiling target protons were identified by their time of flight and energy loss in a detector (RPD) which consisted of two cylindrical rings of scintillating counters at distances of 12 cm and 78 cm from the beam axis, covering the polar angle range above  $50^\circ$  as seen from the target centre. The angular range between the RPD and the opening angle of the spectrometer of about  $\pm 10^\circ$  was covered mostly by a large-area photon and charged-particle veto detector (SW), thus enriching the data recording with kinematically complete events [16]. The trigger for taking the present data required coincidence between beam definition counters and the RPD, and no veto from the SW nor from a small counter telescope for non-interacting beam particles far downstream (32 m) from the target. A sample of  $4.5 \times 10^9$  events was recorded with this trigger in 2008.

For the analysis of the exclusively produced  $\pi^- \eta$  and  $\pi^- \eta'$  mesonic systems, the  $\eta$  was detected by its decay  $\eta \rightarrow \pi^- \pi^+ \pi^0$  ( $\pi^0 \rightarrow \gamma\gamma$ ), and the  $\eta'$  by its decay  $\eta' \rightarrow \pi^- \pi^+ \eta$  ( $\eta \rightarrow \gamma\gamma$ ). The preselection for the common final state  $\pi^- \pi^- \pi^+ \gamma\gamma$  required

- (a) three tracks with total charge  $-1$  reconstructed in the spectrometer,
- (b) a vertex, located inside the target volume, with one incoming beam particle track and the three outgoing tracks,
- (c) exactly two “eligible” clusters in the electromagnetic calorimeters of COMPASS (ECAL1, ECAL2), and

- (d) the total energy  $E_{\text{tot}}$  of the outgoing particles within a 10 GeV wide window centred on the 6 GeV FWHM peak at 191 GeV in the  $E_{\text{tot}}$  distribution.

Clusters were considered “eligible” if they were not associated with a reconstructed track, if the cluster energy was above 1 GeV and 4 GeV in ECAL1 and ECAL2, respectively, and if their timing with respect to the beam was within  $\pm 4$  ns.

Sharp  $\eta$  ( $\eta'$ ) peaks of widths  $3 \text{ MeV}/c^2$ - $4 \text{ MeV}/c^2$  were obtained in the  $\pi^-\pi^+\pi^0$  and  $\pi^-\pi^+\eta$  mass spectra after kinematic fitting of the  $\gamma\gamma$  systems within  $\pm 20 \text{ MeV}/c^2$  windows about the respective  $\pi^0$  and  $\eta$  masses. For the present four-body analyses of the systems  $\pi^-\pi^-\pi^+\pi^0$  and  $\pi^-\pi^-\pi^+\eta$ , broad windows of  $50 \text{ MeV}/c^2$  width about the  $\eta$  and  $\eta'$  masses were applied to the three-body  $\pi^-\pi^+\pi^0$  and  $\pi^-\pi^+\eta$  systems, respectively. In this way, a common treatment of  $\eta^{(\prime)}$  and the small number of non- $\eta^{(\prime)}$  events becomes possible in the subsequent likelihood fit. No significant deviations from coplanarity (required to hold within  $13^\circ$ ) are observed for the momentum vectors of beam particle, mesonic system and recoil proton, which confirms the exclusivity of the reaction. Details are found in Refs. [17, 18].

In order to account for the acceptance of the spectrometer and the selection procedure, Monte Carlo simulations [15, 19] were performed for four-body phase-space distributions. The latter were weighted with the experimental  $t$  distributions, approximated by  $d\sigma/dt \propto |t| \exp(-b|t|)$  with slope parameter  $b = 8.0 (\text{GeV}/c)^{-2}$  and  $b = 8.45 (\text{GeV}/c)^{-2}$  for  $\eta'\pi^-$  and  $\eta\pi^-$ , respectively. The observed weak mass-dependence of the slope parameter was found not to affect the present results. The overall acceptances for  $\eta\pi^-$  and  $\eta'\pi^-$  in the present kinematic range and decay channels amounted to 10 % and 14 %, respectively. Due to the large coverage of forward solid angle by the COMPASS spectrometer, the acceptances vary smoothly over the relevant regions of phase space, see Ref. [20]. A test of the Monte Carlo description was provided by comparison to a five-charged-track sample where  $\eta'$  decays via  $\pi^+\pi^-\eta$  ( $\eta \rightarrow \pi^+\pi^-\pi^0$ ). The known branching ratio of  $\eta$  decay into  $\gamma\gamma$  and  $\pi^-\pi^+\pi^0$  was reproduced [18] leading to a conservative estimate of 8% for the uncertainty of the relative acceptance of the two channels discussed here.

To visualize the gross features of the two channels, subsamples of events were selected with tight  $\pm 10 \text{ MeV}/c^2$  windows on the  $\eta$  and  $\eta'$  masses. These contain 116 000 and 39 000 events, respectively, including 5% background from non- $\eta^{(\prime)}$  events. These subsamples are shown as function of the  $\eta\pi^-$  and  $\eta'\pi^-$  mass in Figs. 1 (a) and (b), and additionally in the scatter plots Figs. 2 (a) and (b) as a function of these invariant masses and of  $\cos \vartheta_{\text{GJ}}$ , where  $\vartheta_{\text{GJ}}$  is the angle between the directions of the  $\eta^{(\prime)}$  and the beam as seen in the centre of mass of the  $\eta^{(\prime)}\pi^-$  system (polar angle in the Gottfried-Jackson frame). These distributions are integrated over  $|t|$  from  $0.1 (\text{GeV}/c)^2$  to  $1.0 (\text{GeV}/c)^2$  and over the azimuth  $\varphi_{\text{GJ}}$  (measured with respect to the reaction plane). The  $\varphi_{\text{GJ}}$  distributions are observed to follow closely a  $\sin^2 \varphi_{\text{GJ}}$  pattern throughout the mass ranges covered in both channels [18, 20].

Several salient features of the intensity distributions in Fig. 2 are noted before proceeding to the partial-wave analysis. In the  $\eta\pi^-$  data, the  $a_2(1320)$  with its two-hump  $D$ -wave angular distribution is prominent, see also Fig. 1 (a). The  $D$ -wave pattern extends to  $2 \text{ GeV}/c^2$  where interference with the  $a_4(2040)$  can be discerned. For higher masses, increasingly narrow forward/backward peaks are observed. This feature corresponds to the emergence of a rapidity gap. In terms of partial waves it indicates coherent contributions from larger angular momenta. Forward/backward asymmetries (only weakly affected by acceptance) occur for all masses in both channels, which indicates interference of odd and even partial waves. In the  $\eta'\pi^-$  data, the  $a_2(1320)$  is close to the threshold energy of this channel (1.1 GeV), and the signal is not dominant, see also Fig. 1 (b). A forward/backward asymmetric interference pattern, indicating coherent  $D$ - and  $P$ -wave contributions with mass-dependent relative phase, governs the  $\eta'\pi^-$  mass range up to  $2 \text{ GeV}/c^2$ . In the  $a_4(2040)$  region, well-localised interference is recognised. As for  $\eta\pi^-$ , narrow forward/backward peaking occurs at higher mass, but in this case the forward/backward asymmetry is visibly larger over the whole mass range of  $\eta'\pi^-$ .

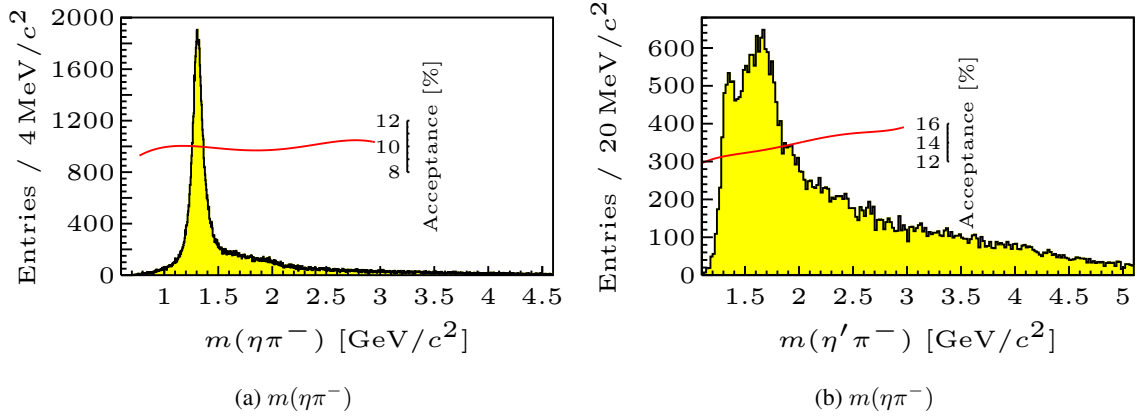


Fig. 1: Invariant mass spectra (not acceptance corrected) for (a)  $\eta\pi^-$  and (b)  $\eta'\pi^-$ . Acceptances (continuous lines) refer to the kinematic ranges of the present analysis.

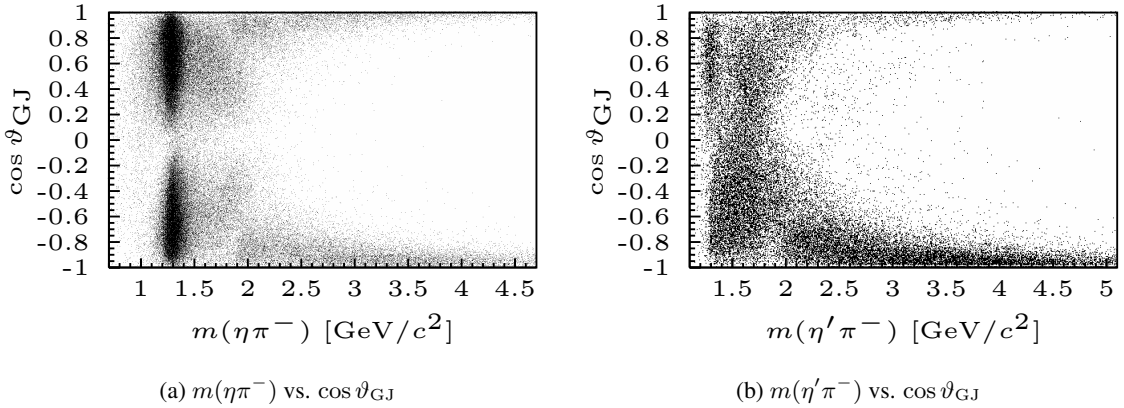


Fig. 2: Data (not acceptance corrected) as a function of the invariant  $\eta\pi^-$  (a) and  $\eta'\pi^-$  (b) mass and of the cosine of the decay angle in the respective Gottfried-Jackson frames where  $\cos\vartheta_{GJ} = 1$  corresponds  $\eta^{(\prime)}$  emission in the beam direction. Two-dimensional acceptances can be found in Ref. [20].

The data were subjected to a partial-wave analysis (PWA) using a program developed at Illinois and VES [21–23]. Independent fits were carried out in  $40\text{ MeV}/c^2$  wide bins of the four-body mass from threshold up to  $3\text{ GeV}/c^2$  (so-called mass-independent PWA). Momentum transfers were limited to the range given above.

An  $\eta^{(\prime)}\pi^-$  partial-wave is characterised by the angular momentum  $L$ , the absolute value of the magnetic quantum number  $M = |m|$  and the reflectivity  $\epsilon = \pm 1$ , which is the eigenvalue of reflection about the production plane. Positive (negative)  $\epsilon$  is chosen to correspond to natural (unnatural) spin-parity of the exchanged Reggeon with  $J_{\text{tr}}^P = 1^-$  or  $2^+$  or  $3^- \dots (0^-$  or  $1^+$  or  $2^- \dots)$  transfer to the beam particle [18, 24]. These two classes are incoherent.

In each mass bin, the differential cross section as a function of four-body kinematic variables  $\tau$  is taken to be proportional to a model intensity  $I(\tau)$  which is expressed in terms of partial-wave amplitudes  $\psi_{LM}^\epsilon(\tau)$ ,

$$I(\tau) = \sum_{\epsilon} \left| \sum_{L,M} A_{LM}^\epsilon \psi_{LM}^\epsilon(\tau) \right|^2 + \text{non-}\eta^{(\prime)} \text{ background.} \quad (1)$$

The magnitudes and phases of the complex numbers  $A_{LM}^\epsilon$  constitute the free parameters of the fit. The expected number of events in a bin is

$$\bar{N} \propto \int I(\tau)a(\tau)d\tau, \quad (2)$$

where  $d\tau$  is the four-body phase space element and  $a(\tau)$  designates the efficiency of detector and selection. Following the extended likelihood approach [24, 25], fits are carried out maximizing

$$\ln \mathcal{L} \sim -\bar{N} + \sum_{k=1}^n \ln I(\tau_k), \quad (3)$$

where the sum runs over all observed events in the mass bin. In this way, the acceptance-corrected model intensity is fit to the data.

The partial-wave amplitudes are composed of two parts: a factor  $f_\eta$  ( $f_{\eta'}$ ) that describes both the Dalitz plot distribution of the successive  $\eta$  ( $\eta'$ ) decay [26] and the experimental peak shape, and a two-body partial-wave factor that depends on the primary  $\eta^{(\prime)}\pi^-$  decay angles. In this way, the four-body analysis is reduced to quasi-two-body. The partial-wave factor for the two spinless mesons is expressed by spherical harmonics. Thus, the full  $\eta(\pi^-\pi^+\pi^0)\pi^-$  partial-wave amplitudes read

$$\begin{aligned} \psi_{LM}^\epsilon(\tau) = & f_\eta(p_{\pi^-}, p_{\pi^+}, p_{\pi^0}) \times Y_L^M(\vartheta_{GJ}, 0) \\ & \times \begin{cases} \sin M\varphi_{GJ} & \text{for } \epsilon = +1 \\ \cos M\varphi_{GJ} & \text{for } \epsilon = -1 \end{cases} \end{aligned} \quad (4)$$

and analogously for  $\eta'(\pi^-\pi^+\eta)\pi^-$ . There are no  $M = 0$ , and therefore no  $L = 0$  waves for  $\epsilon = +1$ . The fits require a weak  $L = M = 0$ ,  $\epsilon = -1$  amplitude which contributes 0.5% (1.1%) to the total  $\eta\pi^-$  ( $\eta'\pi^-$ ) intensity. This isotropic wave is attributed to incoherent background containing  $\eta^{(\prime)}$ , whereas the non- $\eta^{(\prime)}$  background amplitude in Eq. 1 is isotropic in four-body phase space.

An independent two-body PWA was carried out not taking into account the decays of the  $\eta^{(\prime)}$ , but using tight window cuts ( $\pm 10 \text{ MeV}/c^2$ ) on the  $\eta^{(\prime)}$  peak in the respective three-body spectra. The results were found to be consistent with the present analysis [18].

The above-mentioned azimuthal  $\sin^2 \varphi_{GJ}$  dependence is in agreement with a strong  $M = 1$  dominance, as was experienced earlier [6–9]. No  $M > 1$  contributions are needed to fit the data in the present  $t$  range, with the exception of the  $\eta\pi^-$   $D$ -wave where statistics allows the extraction of a small  $M = 2$  contribution. The final fit model is restricted to the coherent  $L = 1 - 6$ ,  $M = 1$  plus  $L = 2$ ,  $M = 2$  partial waves from natural parity transfer ( $\epsilon = +1$ ) and the incoherent backgrounds introduced above.

Incoherence of partial waves of the same naturality, leading to additional terms in Eq. (1), could arise from contributions with and without proton helicity flip, or from different  $t$ -dependences of the amplitudes over the broad  $t$  range. However, for two pseudoscalars, incoherence or partial incoherence of any two partial waves with  $M = 1$  can be accommodated by full coherence with appropriate choice of phase [7]. Comparing PWA results for  $t$  above and below  $0.3 (\text{GeV}/c)^2$ , no significant variation of the relative  $M = 1$  amplitudes with  $t$  is observed [18]. The  $L = 2$ ,  $M = 2$  contribution shows a different  $t$ -dependence but does not introduce significant incoherence.

In general, a two-pseudoscalar PWA suffers from discrete ambiguities [24, 27, 28]. The observed insignificance of unnatural-parity transfer crucially reduces the ambiguities. In the case of  $\eta\pi^-$ , the remaining ambiguities are resolved when the  $M = 2$   $D$ -wave amplitude is introduced. For  $\eta'\pi^-$ , ambiguities occur when the PWA is extended beyond the dominant  $L = 1, 2$  and  $4$  waves. We resolve this by requiring continuous behaviour of the dominant partial waves and of the Barrelet zeros [24]. The

acceptable solutions agree within the statistical uncertainties with the solution selected here, which is the one with the smallest  $L = 3$  contribution.

The results of the PWA are presented as intensities of all included partial waves in Figs. 3, 4, and as relative phases with respect to the  $L = 2, M = 1$  wave in Fig. 5. The plotted intensities are the acceptance-corrected numbers of events in each mass bin, as derived from the  $|A_{LM}^c|^2$  of Eq. 1. Feedthrough of the order of 3% from the dominant  $a_2(1320)$  signal is observed in the  $L = 4 \eta\pi^-$  distribution, as shown in light colour in Fig. 3. Relative intensities integrated over mass up to  $3 \text{ GeV}/c^2$ , taking into account the respective  $\eta^{(\prime)}$  decay branchings, are given in Table 1. The ratio of the summed intensities is  $I(\eta\pi^-)/I(\eta'\pi^-) = 4.0 \pm 0.3$ . This ratio is not affected by luminosity, its error is estimated from the uncertainty of the acceptance. The  $\eta\pi^-$  yield is larger for all even- $L$  waves. Conversely, the odd- $L$  yields are larger in the  $\eta'\pi^-$  data.

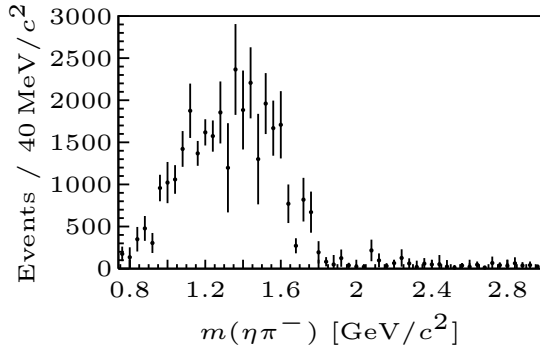
The  $\eta\pi^-$   $P$ -wave intensity shows a compact peak of  $400 \text{ MeV}/c^2$  width, centred at a mass of  $1.4 \text{ GeV}/c^2$ . Beyond  $1.8 \text{ GeV}/c^2$  it disappears. The  $D$ -wave intensity is a factor of twenty larger than the  $P$ -wave intensity. These observations resemble those at lower beam energy [7, 9]. A similar  $P$ -wave peak was observed in  $\bar{p}n$  annihilation at rest, where it appears with an intensity comparable to that of the  $D$ -wave [29]. The present  $D$ -wave is characterised by a dominant  $a_2(1320)$  peak and a broad shoulder that extends to higher masses and possibly contains the  $a_2(1700)$ . An  $M = 2$   $D$ -wave intensity is found at the 5% level. The  $G$ -wave shows a peak consistent with the  $a_4(2040)$  and a broad bump centred at about  $2.7 \text{ GeV}/c^2$ . The  $F, H$  and  $I$ -waves ( $L = 3, 5, 6$ ) adopt each less than 1% of the intensity in the present mass range but are significant in the likelihood fit as can be judged from the uncertainties given in Table 1.

The  $\eta'\pi^-$   $P$  and  $D$ -wave have comparable intensities. The former peaks at  $1.65 \text{ GeV}/c^2$ , drops to almost zero at  $2 \text{ GeV}/c^2$  and displays a broad second maximum around  $2.4 \text{ GeV}/c^2$ . The  $D$ -wave shows a two-part structure similar to  $\eta\pi^-$  but with relatively larger intensity of the shoulder. The  $G$ -wave distribution shows an  $a_4(2040)$  plus bump shape as observed for  $\eta\pi^-$ . In contrast to the  $G$  and  $I$ -waves, the odd  $F$  and  $H$ -waves have an order of magnitude more relative intensity than in the  $\eta\pi^-$  data. The  $F$ -wave distribution features a broad peak around  $2.6 \text{ GeV}/c^2$ .

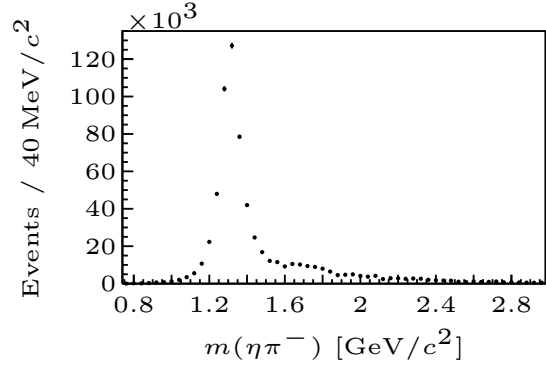
Phase motions in both systems can best be studied with respect to the  $D$ -wave, which is present with sufficient intensity in the full mass range. The rapid phase rotations caused by the  $a_2(1320)$  and  $a_4(2040)$  resonances are discernible. The  $P$  versus  $D$ -wave phases in both systems are almost the same from the  $\eta'\pi^-$  threshold up to  $1.4 \text{ GeV}/c^2$  where a branching takes place. Given the similarity of the  $D$ -wave intensities after applying a kinematical factor (see below), it is suggestive to ascribe the different relative phase motions in the  $1.4 \text{ GeV}/c^2$ - $2.0 \text{ GeV}/c^2$  range to the  $P$ -wave. It is noted that the  $P$ -wave intensities drop dramatically within this region, almost vanishing at  $1.8 \text{ GeV}/c^2$  in  $\eta\pi^-$  and at  $2 \text{ GeV}/c^2$  in  $\eta'\pi^-$ . In contrast, the  $G$ - versus  $D$ -phase motions are almost identical. All phase differences tend to constant values at high masses, which is a wave-mechanical condition for narrow angular focussing.

Fits of resonance and background amplitudes to these PWA results (so-called mass-dependent fits) lead to strongly model-dependent resonance parameters. If these fits are restricted to masses below  $1.9 \text{ GeV}/c^2$ , comparable to previous analyses, a simple model incorporating only  $P$  and  $D$ -wave Breit-Wigner amplitudes and a coherent  $D$ -wave background yields  $\pi_1(1400) \eta\pi^-$  resonance parameters and  $\pi_1(1600) \eta'\pi^-$  resonance parameters consistent with those of Refs. [7–9]. However, the inclusion of higher masses demands additional model amplitudes, in particular additional  $D$ -wave resonances and coherent  $P$ -wave backgrounds. The presence of a coherent background in the  $P$ -wave is suggested by the PWA results in Figs. 3, 4, 5 (a): The vanishing of the intensities around  $2.0 \text{ GeV}/c^2$  is ascribed to destructive interference within this partial wave, and the relatively slow phase motion across the  $\eta'\pi^-$   $P$ -wave peak demands the additional amplitude in order to dampen the  $\pi_1(1600)$  phase rotation. Fitted  $P$ -wave resonance masses in both channels are found to be shifted upwards by typically  $200 \text{ MeV}/c^2$  when introducing constant-phase

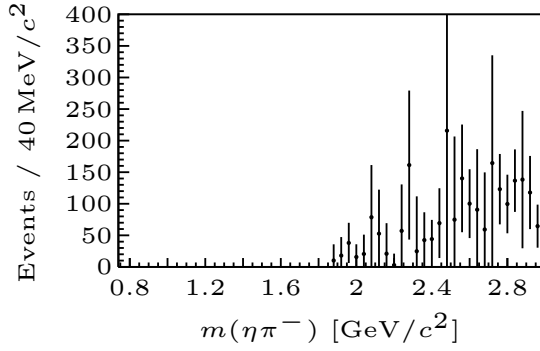




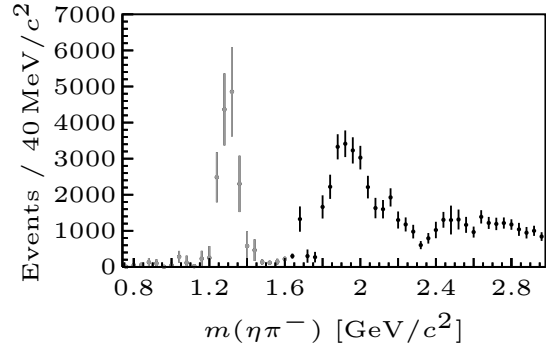
(a)  $P$ -wave,  $L = 1$



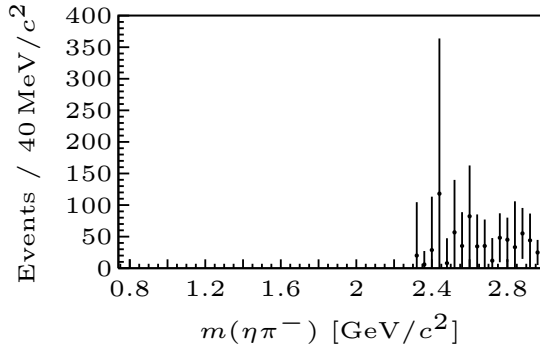
(b)  $D$ -wave,  $L = 2$



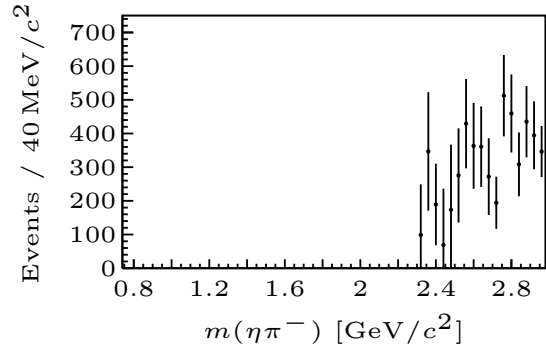
(c)  $F$ -wave,  $L = 3$



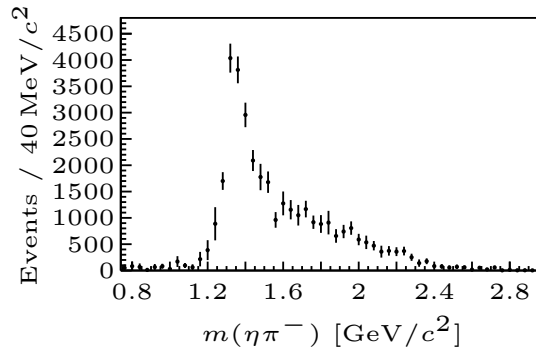
(d)  $G$ -wave,  $L = 4$



(e)  $H$ -wave,  $L = 5$



(f)  $I$ -wave,  $L = 6$



(g)  $D$ -wave,  $L = 2, M = 2$

Fig. 3: Intensities of the  $L = 1 - 6$ ,  $M = 1$  and  $L = 2$ ,  $M = 2$  partial waves from the partial-wave analysis of the  $\eta\pi^-$  data in mass bins of  $40 \text{ MeV}/c^2$  width. The light-colored part of the  $L = 4$  intensity below  $1.5 \text{ GeV}/c^2$  is due to feedthrough from the  $L = 2$  wave. The error bars correspond to a change of the log-likelihood by half a unit and do not include MC fluctuations which are on the order of 5%.

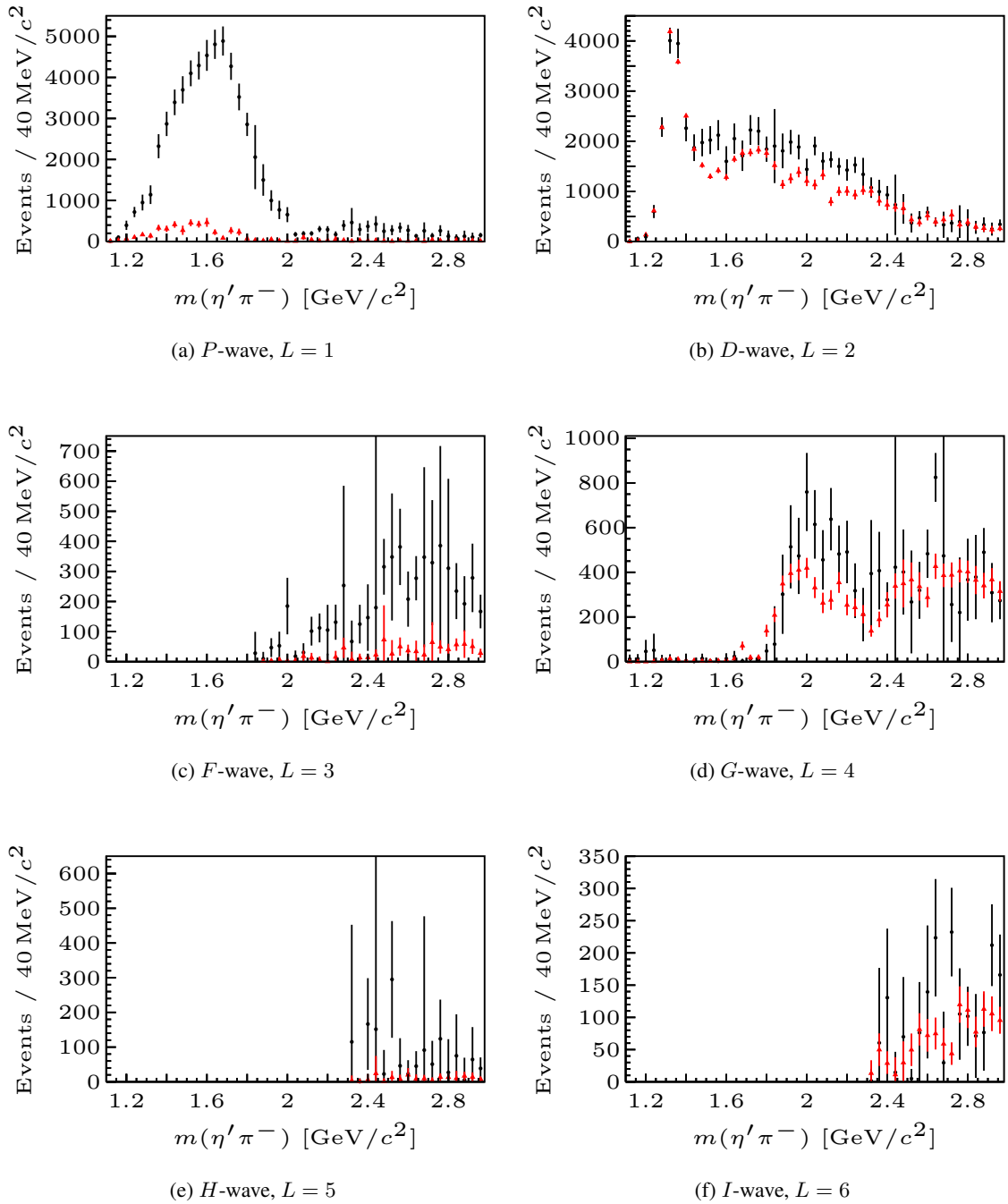


Fig. 4: Intensities of the  $L = 1 - 6$ ,  $M = 1$  partial waves from the partial-wave analysis of the  $\eta' \pi^-$  data in mass bins of  $40 \text{ MeV}/c^2$  width (circles). Shown for comparison (triangles) are the  $\eta \pi^-$  results scaled by the relative kinematical factor given in Eq. (7).

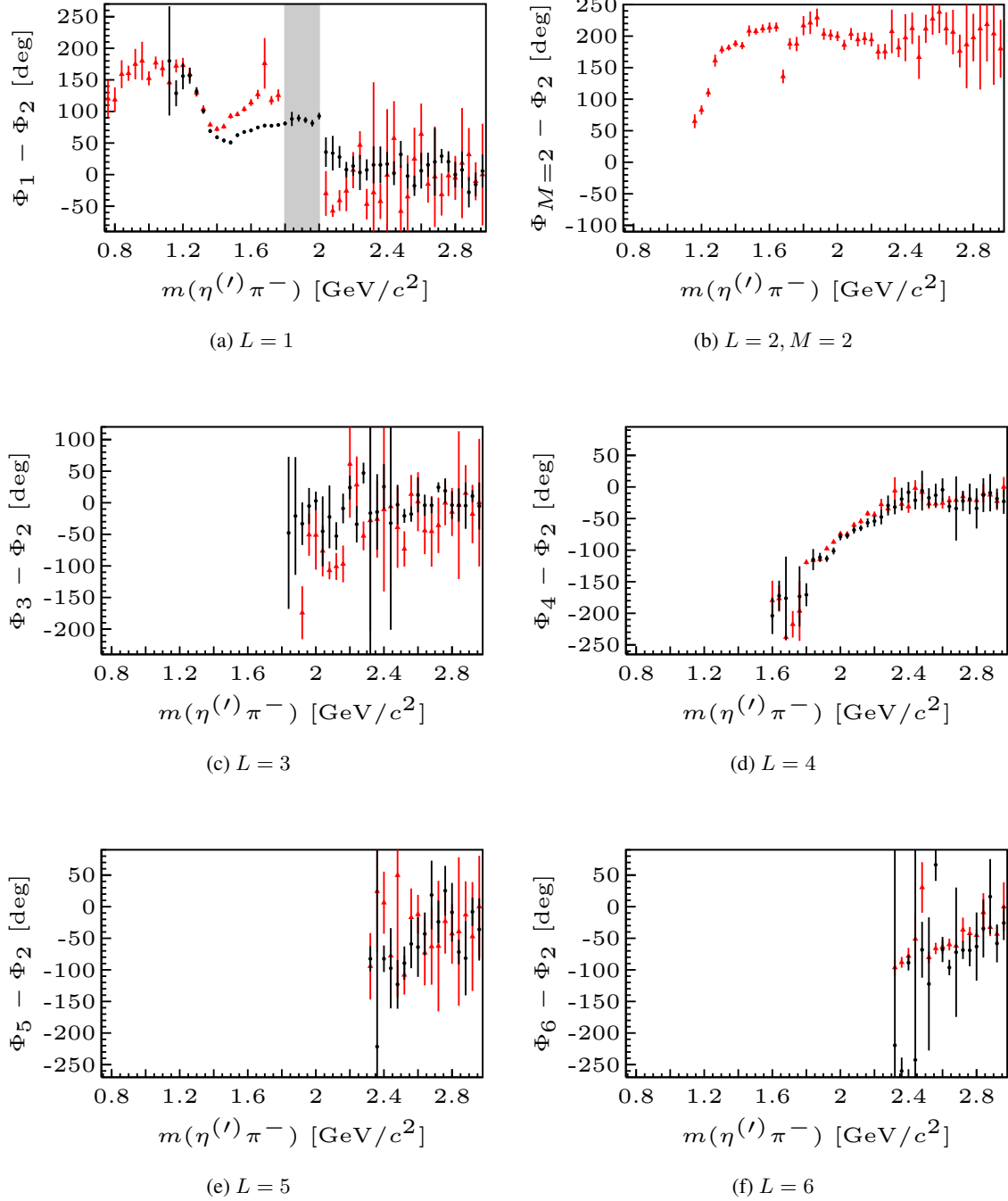


Fig. 5: Phases  $\Phi_L$  of the  $M = 1$  partial waves with angular momentum  $L$  relative to the  $L = 2, M = 1$  wave of  $\eta\pi^-$  (triangles) and  $\eta'\pi^-$  (circles) systems. For  $\eta\pi^-$ , the phase between the  $P$  and  $D$ -waves is ill-defined in the region of vanishing  $P$ -wave intensity between 1.8 and 2.05  $\text{GeV}/c^2$  (shaded). Panel (b) shows the relative  $M = 2$  versus  $M = 1$  phase of the  $\eta\pi^-$   $D$ -wave.

model backgrounds as in Ref. [23]. In the present Letter, we refrain from proposing resonance parameters for the exotic  $P$ -wave or even the exotic  $F$  and  $H$ -waves observed here. The present observations at masses beyond the  $a_2(1320)$  and the  $\pi_1$  structures might stimulate extensions of resonance-production models, as e.g. multi-Regge models [13].

For the distinct  $a_2(1320)$  and  $a_4(2040)$  resonances, mass-dependent fits using a standard relativistic Breit-Wigner parameterisation, which for the  $a_2$  includes also the  $\rho\pi$  decay in the parameterisation of the total width [6], give the following results:

$$\begin{aligned}
m(a_2) &= 1315 \pm 12 \text{ MeV}/c^2, & \Gamma(a_2) &= 119 \pm 14 \text{ MeV}/c^2, \\
m(a_4) &= 1900^{+80}_{-20} \text{ MeV}/c^2, & \Gamma(a_4) &= 300^{+80}_{-100} \text{ MeV}/c^2, \\
B_2 &\equiv \frac{N(a_2 \rightarrow \eta'\pi^-)}{N(a_2 \rightarrow \eta\pi)} = (5 \pm 2)\%, \\
B_4 &\equiv \frac{N(a_4 \rightarrow \eta'\pi^-)}{N(a_4 \rightarrow \eta\pi)} = (23 \pm 7)\%.
\end{aligned} \tag{5}$$

Here,  $N$  stands for the integrated Breit-Wigner intensities of the given decay branches. The errors given above are dominated by the systematic uncertainty, which is estimated by comparing fits with and without coherent backgrounds,  $a_2(1700)$  or  $\pi_1(1400)$ . The masses and  $B_2$  agree with the PDG values [26]. The decay branching ratio  $B_4$  is extracted here for the first time.

Table 1: Intensities (yields), integrated over the mass range up to  $3 \text{ GeV}/c^2$ , for the partial waves with  $M = 1$  (and  $M = 2$  for  $L = 2$ ) relative to  $L = 2, M = 1$  in  $\eta\pi^-$  (set to 100). These yields take into account the decay branching ratios of  $\eta^{(\prime)}$  into  $\pi^-\pi^+\gamma\gamma$ . Errors are derived from the log-likelihood fit and do not include the common uncertainty (8%) of the acceptance ratio of the two channels. The last column lists  $\eta\pi^-$  over  $\eta'\pi^-$  yield ratios derived from the scaled intensities (see text, Eq. (8)). The first (second) value of  $R_L$  corresponds to range parameter  $r = 0 \text{ fm}$  ( $r = 0.4 \text{ fm}$ ).

$L$	yield ( $\eta\pi^-$ )	yield ( $\eta'\pi^-$ )	$R_L$
1	$5.4 \pm 0.3$	$12.8 \pm 0.4$	$0.08 - 0.12$
2	100 (fixed)	$13.0 \pm 0.3$	$0.84 - 1.18$
2, $M = 2$	$5.4 \pm 0.2$		
3	$0.39 \pm 0.07$	$1.14 \pm 0.13$	$0.14 - 0.19$
4	$10.0 \pm 0.3$	$2.57 \pm 0.18$	$0.80 - 0.97$
5	$0.12 \pm 0.04$	$0.28 \pm 0.10$	$0.13 - 0.15$
6	$0.87 \pm 0.08$	$0.36 \pm 0.05$	$0.66 - 0.74$

For a detailed comparison of the results from the mass-independent PWA of both channels, their different phase spaces and angular-momentum barriers are taken into account. For the decay of pointlike particles, transition rates are expected to be proportional to

$$g(m, L) = q(m) \times q(m)^{2L} \tag{6}$$

with break-up momentum  $q(m)$  [30–32]. Overlaid on the PWA results for  $\eta'\pi^-$  in Fig. 4 are those for  $\eta\pi^-$ , multiplied in each bin by the relative kinematical factor

$$c(m, L) = b \times \frac{g'(m, L)}{g(m, L)}, \tag{7}$$

where  $g^{(\prime)}$  refers to  $\eta^{(\prime)}\pi^-$  with break-up momentum  $q^{(\prime)}$ , and the factor  $b = 0.746$  accounts for the decay branchings of  $\eta$  and  $\eta'$  into  $\pi^-\pi^+\gamma\gamma$  [26].

By integrating the invariant mass spectra of each partial wave, scaled by  $[g^{(\prime)}(m, L)]^{-1}$ , from the  $\eta'\pi^-$  threshold up to  $3 \text{ GeV}/c^2$ , we obtain scaled yields  $I_L^{(\prime)}$  and derive the ratios

$$R_L = b \times I_L/I_L' \quad (8)$$

As an alternative to the angular-momentum barrier factors  $q(m)^{2L}$  of Eq. (6), we have also used Blatt-Weisskopf barrier factors [33]. For the range parameter involved there, an upper limit of  $r = 0.4 \text{ fm}$  was deduced from systematic studies of tensor meson decays, including the present channels [30, 31], whereas for  $r = 0 \text{ fm}$  Eq. (6) is recovered. To demonstrate the sensitivity of  $R_L$  on the barrier model, the range of values corresponding to these upper and lower limits is given in Table 1.

The comparison in Fig. 4 reveals a conspicuous resemblance of the even- $L$  partial waves of both channels. This feature remains if  $r = 0.4 \text{ fm}$ , but the values of  $R_L$  increase with increasing  $r$  (Table 1). This similarity is corroborated by the relative phases as observed in Figs. 5 (d) and (f). The observed behaviour is expected from a quark-line picture where only the non-strange components  $n\bar{n}$  ( $n = u, d$ ) of the incoming  $\pi^-$  and the outgoing system are involved. The similar values of  $R_L$  for  $L = 2, 4, 6$  suggest that the respective intermediate states couple to the same flavour content of the outgoing system.

The quark-line estimate (see Eq. (3) in [31]) for the  $a_2(1320)$  decay branching using  $r = 0.4 \text{ fm}$  and the isoscalar mixing angle in the quark flavour basis,  $\phi = 39.3^\circ$  [32], is  $B_2 = 3.9\%$  for our mass value. This is in reasonable agreement with the present measurement. An analogous calculation for the  $a_4(2040)$  yields  $B_4 = 11.8\%$ , which is below the experimental value. A larger range parameter  $r$  would improve the agreement.

On the other hand, the odd- $L$   $\eta'\pi^-$  intensities are enhanced by a factor 5 – 10 as compared to  $\eta\pi^-$ , see Fig. 4, Table 1. The  $P$ -wave fits well into the trend observed for the  $F$  and  $H$ -waves, which also carry exotic quantum numbers. It is suggestive to ascribe these observations to the dominant  $\mathbf{8} \otimes \mathbf{8}$  and  $\mathbf{1} \otimes \mathbf{8}$  character of the  $\eta\pi^-$  and  $\eta'\pi^-$   $SU(3)_{\text{flavour}}$  configurations, respectively. When the former couples to an octet intermediate state, Bose symmetry demands even  $L$ , whereas the latter may couple to the non-symmetric odd- $L$  configurations. The importance of this relation was already pointed out in previous discussions of the exotic  $\pi_1$ , where in particular the hybrid ( $gq\bar{q}$ ) or the lowest molecular state ( $q\bar{q}q\bar{q}$ ) have  $\mathbf{1} \otimes \mathbf{8}$  character [3–5].

A  $P$ -wave peak, consistent with quoted resonance parameters [26], appears in each channel. In the  $\eta'\pi^-$  channel, its relatively large contribution is directly visible in Fig. 2(b). The forward/backward asymmetry, ascribed to  $L = 1, 3, 5$  amplitudes interfering with the even- $L$  ones, extends to higher masses, where a transition to rapidity-gap phenomena (central production) is expected. In the  $\eta\pi^-$  data, the asymmetry is much less pronounced.

In conclusion, two striking features characterise the systematic behaviour of partial waves presented here:

- (i) The even partial waves with  $L = 2, 4, 6$  show a close similarity between the two channels, both in the intensities as function of mass – after scaling by the phase-space and barrier factors – as well as in their phase behaviour.
- (ii) The odd partial waves with  $L = 1, 3, 5$ , carrying non- $q\bar{q}$  quantum numbers, are suppressed in  $\eta\pi^-$  with respect to  $\eta'\pi^-$ , underlining the importance of flavour symmetry.

## Acknowledgements

We gratefully acknowledge the support of the CERN management and staff as well as the skills and efforts of the technicians of the collaborating institutions. This work was made possible by the financial support of our funding agencies.

## References

### References

- [1] E. Klempt, A. Zaitsev, Glueballs, Hybrids, Multiquarks. Experimental facts versus QCD inspired concepts, *Phys. Rept.* 454 (2007) 1–202. arXiv:hep-ph/0708.4016, doi:10.1016/j.physrep.2007.07.006.
- [2] N. Brambilla, et al., QCD and strongly coupled gauge theories: challenges and perspectives, to be submitted to EPJCarXiv:1404.3723.
- [3] F. Close, H. Lipkin, New Experimental Evidence for Four Quark Exotics: the Serpukhov  $\phi\pi$  Resonance and the GAMS  $\eta\pi$  Enhancement, *Phys. Lett. B*196 (1987) 245–250. doi:10.1016/0370-2693(87)90613-7.
- [4] F. Iddir, et al.,  $q\bar{q}g$  hybrid and  $qq\bar{q}\bar{q}$  diquonium interpretation of the GAMS  $1^{-+}$  resonance, *Phys.Lett. B*205 (1988) 564–568. doi:10.1016/0370-2693(88)90999-9.
- [5] S. U. Chung, E. Klempt, J. G. Körner, SU(3) classification of p-wave  $\eta\pi$  and  $\eta'\pi$  systems, *Eur. Phys. J. A*15 (2002) 539–542. arXiv:hep-ph/0211100, doi:10.1140/epja/i2002-10058-0.
- [6] G. Beladidze, et al., Study of  $\pi^- N \rightarrow \eta\pi^- N$  and  $\pi^- N \rightarrow \eta'\pi^- N$  reactions at 37 GeV/c, *Phys. Lett. B*313 (1993) 276–282. doi:10.1016/0370-2693(93)91224-B.
- [7] S. Chung, et al., Evidence for exotic  $J^{PC} = 1^{-+}$  meson production in the reaction  $\pi^- p \rightarrow \eta\pi^- p$  at 18 GeV/c, *Phys. Rev. D*60 (1999) 092001. arXiv:hep-ex/9902003, doi:10.1103/PhysRevD.60.092001.
- [8] E. I. Ivanov, et al., Observation of exotic meson production in the reaction  $\pi^- p \rightarrow \eta'\pi^- p$  at 18 GeV/c, *Phys. Rev. Lett.* 86 (2001) 3977–3980. arXiv:hep-ex/0101058, doi:10.1103/PhysRevLett.86.3977.
- [9] V. Dorofeev, et al., The  $J^{PC} = 1^{-+}$  hunting season at VES, *AIP Conf. Proc.* 619 (2002) 143–154. arXiv:hep-ex/0110075, doi:10.1063/1.1482444.
- [10] A. Donnachie, P. Page, Interpretation of experimental  $J^{PC}$  exotic signals, *Phys. Rev. D*58 (1998) 114012. arXiv:hep-ph/9808225, doi:10.1103/PhysRevD.58.114012.
- [11] A. Szczepaniak, M. Swat, A. Dzierba, S. Teige,  $\eta\pi$  and  $\eta'\pi$  Spectra and Interpretation of Possible Exotic  $J^{PC} = 1^{-+}$  Mesons, *Phys. Rev. Lett.* 91 (2003) 092002. arXiv:hep-ph/0304095, doi:10.1103/PhysRevLett.91.092002.
- [12] S. Donnachie, H. G. Dosch, O. Nachtmann, P. Landshoff, *Pomeron Physics and QCD*, Camb. Monogr. Part. Phys. Nucl. Phys. Cosmol., Cambridge University Press, 2002.
- [13] T. Shimada, A. Martin, A. Irving, Double regge exchange phenomenology, *Nucl. Phys. B*142 (1978) 344. doi:10.1016/0550-3213(78)90209-2.

- [14] P. Abbon, et al., The COMPASS Experiment at CERN, Nucl. Inst. Meth. A577 (2007) 455–518. arXiv:hep-ex/0703049, doi:10.1016/j.nima.2007.03.026.
- [15] M. Alekseev, et al., The COMPASS 2008 Spectrometer, to be submitted to Nucl. Instr. and Meth. A (2014).
- [16] T. Schlüter, et al., Large-Area Sandwich Veto Detector with WLS Fibre Readout for Hadron Spectroscopy at COMPASS, Nucl. Inst. and Meth. A654 (2011) 219. arXiv:1108.4587, doi:10.1016/j.nima.2011.05.069.
- [17] T. Schlüter, The exotic  $\eta'\pi^-$  Wave in 190 GeV  $\pi^-p \rightarrow \pi^-\eta'p$  at COMPASS, in: B. Grube, S. Paul, N. Brambilla (Eds.), Proceedings of the XIV International Conference on Hadron Spectroscopy, eConf C110613, 2011. arXiv:1108.6191. URL <http://www.slac.stanford.edu/econf/C110613>
- [18] T. Schlüter, The  $\pi^-\eta$  and  $\pi^-\eta'$  systems in exclusive 190 GeV  $\pi^-p$  reactions at COMPASS (CERN), Ph.D. thesis, Ludwig-Maximilians-Universität, München (2012). URL <http://www.compass.cern.ch/compass/publications/theses/%2012%5Fphd%5Fschlueter.pdf>
- [19] CERN, GEANT – Detector Description and Simulation Tool (October 1994).
- [20] T. Schlüter, Odd and Even Partial Waves of  $\eta\pi^-$  and  $\eta'\pi^-$  in 191 GeV  $\pi^-p$ , PoS(Hadron 2013) 085. arXiv:1401.4067.
- [21] G. Ascoli, et al., Partial Wave Analysis of the  $3\pi$  Decay of the  $A_2$ , Phys. Rev. Lett. 25 (1970) 962. doi:10.1103/PhysRevLett.25.962.
- [22] I. Karchaev, D. Ryabchikov, private communication.
- [23] M. Alekseev, et al., Observation of a  $J^{PC} = 1^{-+}$  exotic resonance in diffractive dissociation of 190 GeV/c  $\pi^-$  into  $\pi^-\pi^-\pi^+$ , Phys. Rev. Lett. 104 (2010) 241803. arXiv:0910.5842, doi:10.1103/PhysRevLett.104.241803.
- [24] S. U. Chung, Techniques of amplitude analysis for two pseudoscalar systems, Phys. Rev. D56 (1997) 7299–7316. doi:10.1103/PhysRevD.56.7299.
- [25] R. Barlow, Extended maximum likelihood, Nucl. Inst. Meth. A297 (3) (1990) 496 – 506. doi:10.1016/0168-9002(90)91334-8.
- [26] J. Beringer, et al., Review of Particle Physics, Phys.Rev. D86 (2012) 010001. doi:10.1103/PhysRevD.86.010001.
- [27] A. Martin, et al., A Study of Isospin 1 Meson States Using 10 GeV/c  $K^-K^0$  Production Data, Phys. Lett. B74 (1978) 417. doi:10.1016/0370-2693(78)90693-7.
- [28] S. Sadovsky, On the ambiguities in the partial wave analysis of  $\pi^-p \rightarrow \eta\pi^0n$  reaction, Tech. rep., IHEP 91-75, IHEP Protvino (1991).
- [29] A. Abele, et al., Exotic  $\eta\pi$  state in  $\bar{p}d$  annihilation at rest into  $\pi^-\pi^0\eta p_{\text{spectator}}$ , Phys. Lett. B423 (1998) 175–184. doi:10.1016/S0370-2693(98)00123-3.
- [30] K. Peters, E. Klempt, The suppression of  $s\bar{s}$  pair creation from tensor meson decays, Phys.Lett. B352 (1995) 467–471. doi:10.1016/0370-2693(95)00457-V.
- [31] A. Abele, et al., Study of the  $\pi^0\pi^0\eta'$  final state in  $\bar{p}p$  annihilation at rest, Phys. Lett. B404 (1997) 179–186. doi:10.1016/S0370-2693(97)00526-1.

- [32] A. Bramon, R. Escribano, M. Scadron, The  $\eta - \eta'$  mixing angle revisited, *Eur. Phys. J. C* 7 (1999) 271–278. [arXiv:hep-ph/9711229](https://arxiv.org/abs/hep-ph/9711229), [doi:10.1007/s100529801009](https://doi.org/10.1007/s100529801009).
- [33] F. von Hippel, C. Quigg, Centrifugal-barrier effects in resonance partial decay widths, shapes, and production amplitudes, *Phys. Rev. D* 5 (1972) 624–638. [doi:10.1103/PhysRevD.5.624](https://doi.org/10.1103/PhysRevD.5.624).